response pattern with and without priming burst stimulation at both stimulation intensity was same (100 μA; **Figures 4F,G**). Application of gabazine enhanced the response in the control condition (−burst; **Figures 4C,G**), but burst stimulation failed to induce facilitation in the presence of GABA$_A$ receptor inhibitors (**Figures 4D,I**; priming burst 100 μA). That is also true if the stimulation intensity of the priming burst was lowered to 40 μA (**Figures 4E,J,K**) where the priming burst stimulation did not saturate the response.

That was clearer in the pooled data (**Figure 5**). The differences caused by the priming burst stimulation were significantly larger at stimulus intensities greater than 100 μA in the stimulus #3 and #4 (**Figures 5D–F**). In presence of gabazine, there were no significant increase in the response caused by the priming burst stimulation (compare open and black filled bars in **Figures 5G–L**). Again that is not due to the saturation effect caused by gabazine, because even in the small stimulus intensity (40 μA) failed to cause the facilitation (compare open and blue filled bars in **Figures 5G–L**), strongly indicating that activation of GABA$_A$-receptors is a critical factor in PBF. It is interesting to note that in presence of gabazine priming burst tend to reduce the following response (significant decrease only seen in **Figure 5H** #1 stimilus open and black bars).

Transient E-S Augumentation Without a Decrease in Spike Generation Threshold

We next examined if the E-S augumenation induced by the priming burst stimulation accompanied modifications of spike generation threshold in postsynaptic cells. The threshold for spike generation was examined by directly injecting current into pyramidal cells through a fine tipped intracellular electrode with or without priming synaptic burst stimulation (**Figures 6A,B**). When the priming burst stimulation was given 170 ms before the current injection like in the case of PBS, number of the spikes caused by the injected current were suppressed (**Figure 6C** open circle) compared to those without priming burst (**Figure 6C** close circle). The membrane potential that induce the first action potential was significantly lower in the control than with priming burst (**Figure 6D**) That led us to confirm an increase in spike generation threshold (**Figure 6C**), indicating that greater postsynaptic excitability is not the cause of PBS induced E-S augmentation.

DISCUSSION

In the present study, we showed that a pair of 100 Hz brief burst stimulations (PBS) to the Schaffer collateral afferent induced a transient facilitation of the postsynaptic response (PBF) in the intracellular recordings and VSD optical recordings in the area CA1 of rat hippocampal slices in the presence of an NMDA blocker. Since the same PBS did not cause the facilitation of EPSC under a voltage-clamp condition, PBF was not caused by the change in presynaptic nor the postsynaptic-receptor modification. The PBF accompanied the increase in the EPSP-spike (E-S) coupling. This short-term modification of E-S coupling was seen when the priming burst of the PBS consisted of more than three and the interburst frequency was 150 ms. The optimal stimulation pattern was close to the TBS that originally aimed to mimic the natural oscillatory activity of the hippocampus (Larson and Lynch, 1986; Larson et al., 1986). The PBF was abolished when the GABAergic inhibitory circuit was blocked by the application of gabazine and did not accompany the lowering of the spike threshold of the postsynaptic cells. Taken together the PBF is a short-term plastic facilitation of excitation and E-S coupling of the postsynaptic pyramidal cells of area CA1 caused by transient modification of GABAergic systems. These results imply that CA1 neural circuit equips the theta-dependent amplifier that specifically amplified spike generation to the theta-gamma combined activity. In other words, the PBF could be a part of the key mechanism that enable CA1 to decode the theta oscillatory neural signal as a meaningful signal.

Comparison with the Paired-Pulse Facilitation (PPF) and the E-S Potentiation

The PBF is a short-term activity modification as is the representative short-term plasticity PPF that occurs when a pair of a stimuli were given to same afferent in rapid (intervals less than 100–200 ms) succession (Creager et al., 1980; McNaughton, 1980, 1982). In the case of the PPF, it is well established that the presynaptic mechanism contributes to the causing it (Manabe et al., 1993; Schulz et al., 1995; Debanne et al., 1996). Although PPF involves GABAergic contribution (Davies et al., 1990, 1991), PBF should be different from PPF in at least two aspects. Firstly the range of the time-window is longer than that in PPF. PBF has a peak at 150 ms (**Figure 3**) while PPF is at 30–60 ms (Creager et al., 1980; McNaughton, 1980, 1982). Secondly, PPF could be observed in the EPSC (Manabe et al., 1993) but PBF could not (**Figure 1**). Hence, the PBF and the PPF are both short-term modifications of neuronal response but should be caused by different mechanisms, at least, in part.

The PBF accompanied a transient increase in E-S coupling. A long-term modification of E-S coupling is well known as an E-S potentiation that is complementary to the induction of LTP (Andersen et al., 1980; Abraham et al., 1987; Chavez-Noriega et al., 1990) and was already noted on the first report of LTP (Bliss and Lømo, 1973). The E-S potentiation (and E-S depression) is a long-term modification of E-S relationship induced by tetanic stimulation and other forms of stimulation (Pugliese et al., 1994; review by Daoudal and Debanne, 2003). Both the modification of intrinsic neuronal excitability of postsynaptic neurons and the modification, including the GABAergic system are responsible for the E-S potentiation and E-S depression depending on the induction condition of LTP (Chavez-Noriega et al., 1989, 1990; Hess and Gustafsson, 1990; Jester et al., 1995; Lu et al., 2000; Daoudal et al., 2002; Marder and Buonomano, 2003; Staff and Spruston, 2003). While PBF did not accompany a lowering of spike threshold (**Figure 6**), GABAergic mechanisms that cause the long-term modification of neural response that resulted in E-S potentiation can apply to the cause of PBF (see **Figures 4, 5**). However, thinking about

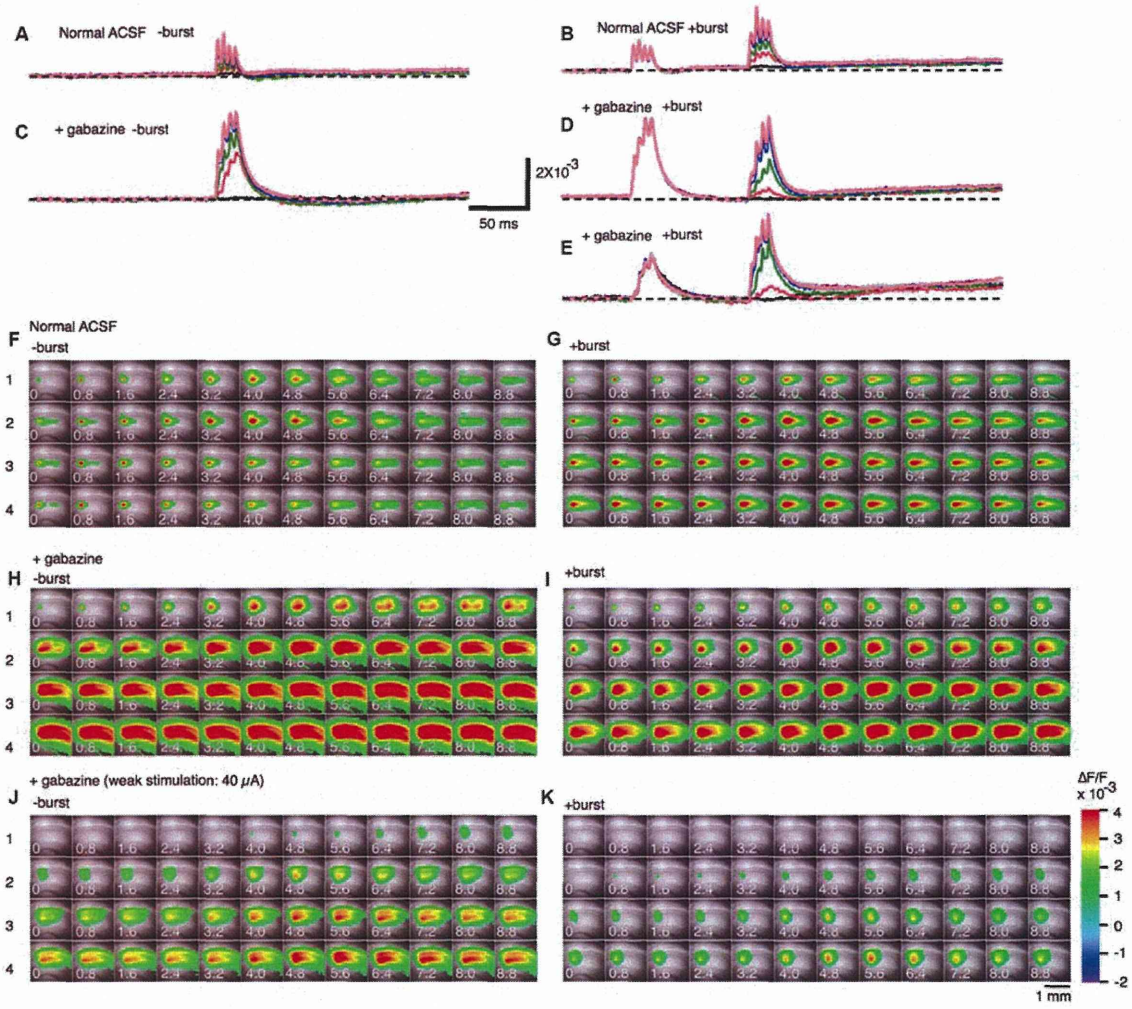

FIGURE 4 | Effect of a GABA$_A$ receptor antagonist (gabazine) on paired burst facilitation. (A–D) Representative traces of optical signals observed upon burst stimulation at different stimulus intensities with (**A,C**; +burst) or without (**B,D**; −burst) a priming burst stimulation (100 μA) in normal ACSF **(A,B)** and in the presence of 10 μM gabazine **(C,D)**. **(E)** The stimulus intensity of a priming burst stimulation was reduced to 40 μA. The test burst stimulation were 20, 40, 60, 100, 150, 200 and 250 μA. **(F–K)** Sets of consecutive images of optical signals sampled every 0.8 ms for the priming burst stimulation **(F,H,J)** and the test burst stimulation burst **(G,I,K)** of stimulation numbers 1–4 (top to bottom). The stimulation intensity of both priming and test burst stimulation were 100 μA in **(F–I)**, while were 40 μA in **(J,K)**. The response **(H–K)** are taken in the presence of 10 μM gabazine. Small numbers on each consecutive images are time from the starting of each stimulation of a brief burst stimulation (1–4) (ms).

a large difference between short-term and long-term neural modification, the way of involvements of these mechanisms should be different.

How Does GABA$_A$-Receptor-Mediated Network activity Cause Paired Burst Facilitation (PBF)

GABAergic inhibition operates by a variety of mechanisms including hyperpolarization and shunting of postsynaptic cells (Bartos et al., 2007; Mann and Paulsen, 2007; Blaesse et al., 2009). The GABA$_A$-receptor-mediated inhibitory system consists of two kinetically different currents GABA$_{A,fast}$ and GABA$_{A,slow}$ (Pearce, 1993), in diverse types of interneurons (reviewed by Maccaferri and Lacaille, 2003). The time constant for GABA$_{A,fast}$ is around 9 ms and GABA$_{A,slow}$ is around 50 ms (Banks et al., 1998). Those kinetically different GABA$_A$-receptors of different types of interneurons are thought to be essential to support nested activity of theta and gamma frequencies (Banks et al., 2000; White et al., 2000; Bartos et al., 2002, 2007). The optimal interburst interval of 150 ms in the present data may imply other processes that should explain a little bit longer time constants than GABA$_{A,slow}$. In this connection, it is interesting to note that

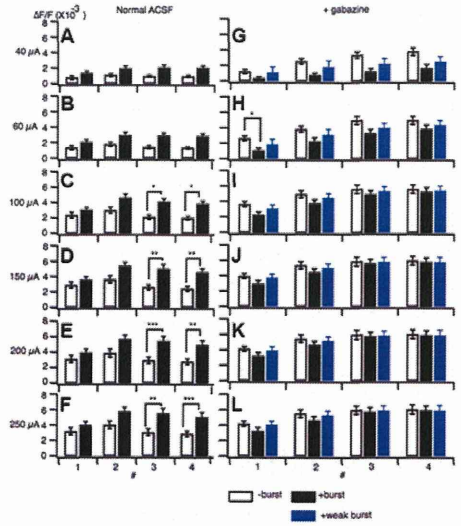

FIGURE 5 | Amplitude of responses at different stimulus intensities without a burst stimulation (open bars) and with a priming burst stimulation (filled bars) in normal ACSF (A–F) and in the presence of gabazine (G–L). The stimulation intensity of a priming burst was 100 μA for black bars, and 40 μA for blue bars in **(G–L)**. (mean ± SEM; $*p < 0.05$, $**p < 0.01$, $***p < 0.001$; $n = 7$).

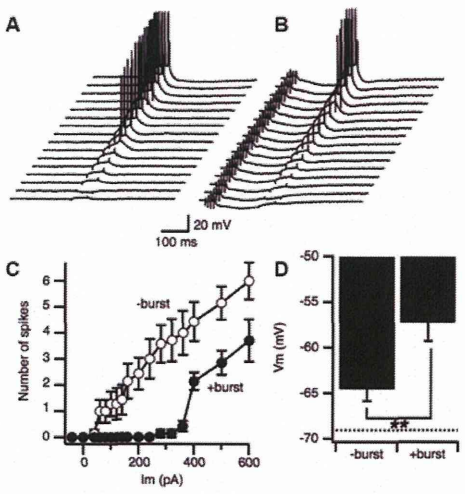

FIGURE 6 | Neuronal excitability was not increased by a priming burst stimulation. (A) Set of traces of intracellular recordings with a sharp intracellular electrode at different amplitudes elicited by a square constant current injection. **(B)** Matching series of traces recorded with a priming synaptic burst stimulation before the constant current injection. **(C)** Number of spikes produced during the current injection without burst stimulation (open circle) and with burst stimulation (filled circle) as a function of the amplitude of the current. Bars represents SEM ($n = 6$ for both groups). **(D)** Membrane potential of the first appearance of spikes when the intensity of injection current increased in the condition of without a priming burst stimulation (−burst) and with the priming burst stimulation (+burst). Dashed line represents the resting potential (−69.06 ± 1.43; $n = 12$). $**p < 0.01$.

high-frequency stimulation causes long-lasting depolarization instead of hyperpolarization (Kaila et al., 2014b). This form of depolarization is considered to result from a depolarizing response to excess administration of GABA (Nicoll and Alger, 1979) that also induces tonic activation of extrasynaptic GABA$_A$ receptors (Semyanov et al., 2004). Accumulating evidence indicates that the GABA$_A$-receptor mediated depolarizations are closely related to the equilibrium potential of the Cl^- (E_{Cl}) shift, which depends on the activity of cation-chloride cotransporters (Buzsáki et al., 2007; Fiumelli and Woodin, 2007; Blaesse et al., 2009; Kaila et al., 2014b). The shift in ECl caused so called "ionic plasticity" that could provide longer processes than each receptor current (Kaila et al., 2014b). We have previously shown that high-frequency stimulation at 100 Hz caused long-lasting GABA$_A$ receptor-dependent depolarization leading to the inhibition of synaptic transmission followed by a facilitation of neuronal activity transduction (Tominaga et al., 2002; Tominaga and Tominaga, 2010). The short-term plasticity caused by 100 Hz stimulation (duration of 400 ms) occurred in less than a second. Hence, we propose that a brief 100 Hz burst stimulation of TBS and PBS may recruit a process that is causing ionic plasticity. In the present study, we found that long-lasting GABA$_A$ receptor-dependent depolarization induced by PBS did not simply increase the depolarizing response, as indicated by the heightened threshold for spike generation in response to a current injection (**Figure 6**). In addition, there was no evidence for presynaptic modulation by GABA$_A$-receptors (Wakita et al., 2014), as there was no facilitation of EPSCs (**Figure 1**). It is still difficult to explain the raised E-S coupling from these controls of inhibitory systems. However, based on the present results and given that perisomatic feed-forward inhibition by GABA$_A$ receptors controls action potential firing (Freund and Katona, 2007; Tominaga et al., 2009), temporal weakening of feed forward inhibition, i.e., dis-inhibition of feed-forward inhibition, seems a part of an explanation for the present results (Lu et al., 2000).

PBF as an Intrinsic Neural Mechanism Generated by Gamma-Theta Oscillations

The 100 Hz burst stimulation protocol used in the present study can be considered to be a form of high-frequency oscillations (HFO; Engel and da Silva, 2012) in the gamma range. In various brain regions, HFO is often observed together with low-frequency oscillations, such as theta oscillations (Buzsáki and da Silva, 2012). In the hippocampus, gamma-theta interactions are thought to be a crucial computational mechanism for processing neural information (Lisman and Jensen, 2013; Nishida et al., 2014). Theta oscillations have long been known to play an important role in encoding information in neural circuits (Buzsáki, 2005) and in memory consolidation during sleep (Mehta et al., 2002). Control of these spikes in entorhinal-hippocampal connections during slow oscillatory activity is critical for hippocampal function (Ahmed and Mehta, 2009). For instance, projections from the medial entorhinal cortex (MEC) layer III mediate ripple activity in the CA1 (Suh et al., 2011) and

control memory processes in the hippocampus (Yamamoto et al., 2014). Moreover, the timing of spikes during theta oscillations is crucial for computation in the hippocampus, as most notably indicated by the phase precession of spikes related to place cell tuning (O'Keefe and Recce, 1993).

The *in vitro* data presented in this study suggest that the CA1 network has an intrinsic mechanism to control spike firing upon the coherent activation of Schaffer collaterals by theta oscillations. This may be mediated at least in part by dendritic K^+ channels that act as cellular devices that regulate the theta frequency time domain (Watanabe et al., 2002). Our results show that the GABA$_A$-receptor activation induced by bursting synaptic input may additionally regulate neural circuitry within CA1 by enabling more efficient transmission of theta range neural transduction. Spike firing in CA1 pyramidal cells is strictly controlled by neuronal inhibition, mostly via perisomatic GABAergic synapses which are abundant in this region (Thompson and Best, 1989; Tominaga et al., 2009). It however remains to be seen how perisomatic inhibition exerts precise control over spike firing in individual cells. A reasonable explanation for the cellular basis for GABA-dependent spike firing regulation may be intrinsic mechanisms that respond to the oscillatory activity of inputs into the CA1.

LTP Induction by Different Stimuli

The present study confirmed that the TBS induces more spikes during the induction of LTP, than the number of spikes that are inhibited by HFS (Tominaga et al., 2002). In consideration of the classical definition of Hebbian plasticity (Hebb, 1949; Stent, 1973), the physiological importance of spikes for the induction of LTP is quite important. In addition, differences in the forms of LTP (Larson and Munkácsy, 2015) elicited by TBS vs. HFS may owe to different sets of molecular cascades initiated by these two distinct processes (Zhu et al., 2015) or it could be caused by differences in the nature of spikes coincident with the synaptic input (Edelmann et al., 2015). We found that spike generation by TBS was controlled by the GABA system, indicating a potential coupling of interneurons and Schaffer collateral inputs onto postsynaptic cells in the circuit (Buzsáki et al., 2004, 2007). The involvement of inhibitory pathways may be important in establishing variability in the ways in which the network is differentially modified by various LTP induction stimuli. Given that LTP induction is still used to test risk for and dysfunction in many brain disorders and malformations (e.g., risk assessment of chemical factors and genetic backgrounds in Alzheimer's disease), it is important to consider that processes underlying LTP induction may differ according to the type of stimulus.

AUTHOR CONTRIBUTIONS

TT designed research; TT and YT performed research; TT and YT analyzed data; TT wrote the article.

FUNDING

Grant from Ministry of Health, Labour and Welfare (H23-Kagaku-Ippan-004, H27-Kagaku-Ippan-007), JST A-STEP, KAKENHI 24500269, 24240076, 15K00413 to TT.

ACKNOWLEDGMENTS

We thank Dr. Michinori Ichikawa for his kind encouragements and helps during the early phase of the work. We also thank Dr. Riichi Kajiwara for critical reading of the manuscript.

REFERENCES

Abraham, W. C., Gustafsson, B., and Wigström, H. (1987). Long-term potentiation involves enhanced synaptic excitation relative to synaptic inhibition in guinea-pig hippocampus. *J. Physiol.* 394, 367–380. doi: 10.1113/jphysiol.1987.sp016875

Ahmed, O. J., and Mehta, M. R. (2009). The hippocampal rate code: anatomy, physiology and theory. *Trends Neurosci.* 32, 329–338. doi: 10.1016/j.tins.2009.01.009

Andersen, P., Sundberg, S. H., Sveen, O., Swann, J. W., and Wigström, H. (1980). Possible mechanisms for long-lasting potentiation of synaptic transmission in hippocampal slices from guinea-pigs. *J. Physiol.* 302, 463–482. doi: 10.1113/jphysiol.1980.sp013256

Banks, M. I., Li, T. B., and Pearce, R. A. (1998). The synaptic basis of GABA$_{A,slow}$. *J. Neurosci.* 18, 1305–1317.

Banks, M. I., White, J. A., and Pearce, R. A. (2000). Interactions between distinct GABA(A) circuits in hippocampus. *Neuron* 25, 449–457. doi: 10.1016/s0896-6273(00)80907-1

Bartos, M., Vida, I., Frotscher, M., Meyer, A., Monyer, H., Geiger, J. R., et al. (2002). Fast synaptic inhibition promotes synchronized gamma oscillations in hippocampal interneuron networks. *Proc. Natl. Acad. Sci. U S A* 99, 13222–13227. doi: 10.1073/pnas.192233099

Bartos, M., Vida, I., and Jonas, P. (2007). Synaptic mechanisms of synchronized gamma oscillations in inhibitory interneuron networks. *Nat. Rev. Neurosci.* 8, 45–56. doi: 10.1038/nrn2044

Bi, G., and Poo, M. (1998). Synaptic modifications in cultured hippocampal neurons: dependence on spike timing, synaptic strength and postsynaptic cell type. *J. Neurosci.* 18, 10464–10472.

Blaesse, P., Airaksinen, M. S., Rivera, C., and Kaila, K. (2009). Cation-chloride cotransporters and neuronal function. *Neuron* 61, 820–838. doi: 10.1016/j.neuron.2009.03.003

Bliss, T. V. P., and Lømo, T. (1973). Long-lasting potentiation of synaptic transmission in the dentate area of the anaesthetized rabbit following stimulation of the perforant path. *J. Physiol.* 232, 331–356. doi: 10.1113/jphysiol.1973.sp010273

Buzsáki, G. (2002). Theta oscillations in the hippocampus. *Neuron* 33, 325–340. doi: 10.1016/s0896-6273(02)00586-x

Buzsáki, G. (2005). Theta rhythm of navigation: link between path integration and landmark navigation, episodic and semantic memory. *Hippocampus* 15, 827–840. doi: 10.1002/hipo.20113

Buzsáki, G. (2006). *Rhythms of the Brain.* Oxford; New York, NY: Oxford University Press.

Buzsáki, G., and da Silva, F. L. (2012). High frequency oscillations in the intact brain. *Prog. Neurobiol.* 98, 241–249. doi: 10.1016/j.pneurobio.2012.02.004

Buzsáki, G., Geisler, C., Henze, D. A., and Wang, X.-J. (2004). Interneuron diversity series: circuit complexity and axon wiring economy of cortical interneurons. *Trends Neurosci.* 27, 186–193. doi: 10.1016/j.tins.2004.02.007

Buzsáki, G., Kaila, K., and Raichle, M. (2007). Inhibition and brain work. *Neuron* 56, 771–783. doi: 10.1016/j.neuron.2007.11.008

Chavez-Noriega, L. E., Bliss, T. V., and Halliwell, J. V. (1989). The EPSP-spike (E-S) component of long-term potentiation in the rat hippocampal slice is modulated by GABAergic but not cholinergic mechanisms. *Neurosci. Lett.* 104, 58–64. doi: 10.1016/0304-3940(89)90329-7

Chavez-Noriega, L. E., Halliwell, J. V., and Bliss, T. V. (1990). A decrease in firing threshold observed after induction of the EPSP-spike (E-S) component of long-term potentiation in rat hippocampal slices. *Exp. Brain Res.* 79, 633–641. doi: 10.1007/bf00229331

Chen, G., Kolbeck, R., Barde, Y. A., Bonhoeffer, T., and Kossel, A. (1999). Relative contribution of endogenous neurotrophins in hippocampal long-term potentiation. *J. Neurosci.* 19, 7983–7990.

Creager, R., Dunwiddie, T., and Lynch, G. (1980). Paired-pulse and frequency facilitation in the CA1 region of the *in vitro* rat hippocampus. *J. Physiol.* 299, 409–424. doi: 10.1113/jphysiol.1980.sp013133

Daoudal, G., and Debanne, D. (2003). Long-term plasticity of intrinsic excitability: learning rules and mechanisms. *Learn. Mem.* 10, 456–465. doi: 10.1101/lm.64103

Daoudal, G., Hanada, Y., and Debanne, D. (2002). Bidirectional plasticity of excitatory postsynaptic potential (EPSP)-spike coupling in CA1 hippocampal pyramidal neurons. *Proc. Natl. Acad. Sci. U S A* 99, 14512–14517. doi: 10.1073/pnas.222546399

Davies, C. H., Davies, S. N., and Collingridge, G. L. (1990). Paired-pulse depression of monosynaptic GABA-mediated inhibitory postsynaptic responses in rat hippocampus. *J. Physiol.* 424, 513–531. doi: 10.1113/jphysiol.1990.sp018080

Davies, C. H., Starkey, S. J., Pozza, M. F., and Collingridge, G. L. (1991). GABA autoreceptors regulate the induction of LTP. *Nature* 349, 609–611. doi: 10.1038/349609a0

Debanne, D., Guérineau, N. C., and Gähwiler, B. H. (1996). Paired-pulse facilitation and depression at unitary synapses in rat hippocampus: quantal fluctuation affects subsequent release. *J. Physiol.* 491, 163–176. doi: 10.1113/jphysiol.1996.sp021204

Edelmann, E., Cepeda-Prado, E., Franck, M., Lichtenecker, P., Brigadski, T., and Leßmann, V. (2015). Theta burst firing recruits BDNF release and signaling in postsynaptic CA1 neurons in spike-timing-dependent LTP. *Neuron* 86, 1041–1054. doi: 10.1016/j.neuron.2015.04.007

Engel, J., Jr., and da Silva, F. L. (2012). High-frequency oscillations–where we are and where we need to go. *Prog. Neurobiol.* 98, 316–318. doi: 10.1016/j.pneurobio.2012.02.001

Fiumelli, H., and Woodin, M. A. (2007). Role of activity-dependent regulation of neuronal chloride homeostasis in development. *Curr. Opin. Neurobiol.* 17, 81–86. doi: 10.1016/j.conb.2007.01.002

Freund, T. F., and Katona, I. (2007). Perisomatic inhibition. *Neuron* 56, 33–42. doi: 10.1016/j.neuron.2007.09.012

Fries, P., Nikolić, D., and Singer, W. (2007). The gamma cycle. *Trends Neurosci.* 30, 309–316. doi: 10.1016/j.tins.2007.05.005

Hebb, D. O. (1949). *The Organization of Behavior: A Neurophysiological Theory.* New York: John Wiley and Sons.

Hess, G., and Gustafsson, B. (1990). Changes in field excitatory postsynaptic potential shape induced by tetanization in the CA1 region of the guinea-pig hippocampal slice. *Neuroscience* 37, 61–69. doi: 10.1016/0306-4522(90)90192-7

Huerta, P. T., and Lisman, J. E. (1995). Bidirectional synaptic plasticity induced by a single burst during cholinergic theta oscillation in CA1 *in vitro*. *Neuron* 15, 1053–1063. doi: 10.1016/0896-6273(95)90094-2

Jester, J. M., Campbell, L. W., and Sejnowski, T. J. (1995). Associative EPSP–spike potentiation induced by pairing orthodromic and antidromic stimulation in rat hippocampal slices. *J. Physiol.* 484, 689–705. doi: 10.1113/jphysiol.1995.sp020696

Kaila, K., Price, T. J., Payne, J. A., Puskarjov, M., and Voipio, J. (2014a). Cation-chloride cotransporters in neuronal development, plasticity and disease. *Nat. Rev. Neurosci.* 15, 637–654. doi: 10.1038/nrn3819

Kaila, K., Ruusuvuori, E., Seja, P., Voipio, J., and Puskarjov, M. (2014b). GABA actions and ionic plasticity in epilepsy. *Curr. Opin. Neurobiol.* 26, 34–41. doi: 10.1016/j.conb.2013.11.004

Kang, H., Welcher, A. A., Shelton, D., and Schuman, E. M. (1997). Neurotrophins and time: different roles for TrkB signaling in hippocampal long-term potentiation. *Neuron* 19, 653–664. doi: 10.1016/s0896-6273(00)80378-5

Korte, M., Carroll, P., Wolf, E., Brem, G., Thoenen, H., and Bonhoeffer, T. (1995). Hippocampal long-term potentiation is impaired in mice lacking brain-derived neurotrophic factor. *Proc. Natl. Acad. Sci. U S A* 92, 8856–8860. doi: 10.1073/pnas.92.19.8856

Korte, M., Staiger, V., Griesbeck, O., Thoenen, H., and Bonhoeffer, T. (1996). The involvement of brain-derived neurotrophic factor in hippocampal long-term potentiation revealed by gene targeting experiments. *J. Physiol. Paris* 90, 157–164. doi: 10.1016/s0928-4257(97)81415-5

Larson, J., and Lynch, G. (1986). Induction of synaptic potentiation in hippocampus by patterned stimulation involves two events. *Science* 232, 985–988. doi: 10.1126/science.3704635

Larson, J., and Munkácsy, E. (2015). Theta-burst LTP. *Brain Res.* 1621, 38–50. doi: 10.1016/j.brainres.2014.10.034

Larson, J., Wong, D., and Lynch, G. (1986). Patterned stimulation at the theta frequency is optimal for the induction of hippocampal long-term potentiation. *Brain Res.* 368, 347–350. doi: 10.1016/0006-8993(86)90579-2

Lisman, J. E., and Jensen, O. (2013). The θ-γ neural code. *Neuron* 77, 1002–1016. doi: 10.1016/j.neuron.2013.03.007

Lu, Y. M., Mansuy, I. M., Kandel, E. R., and Roder, J. (2000). Calcineurin-mediated LTD of GABAergic inhibition underlies the increased excitability of CA1 neurons associated with LTP. *Neuron* 26, 197–205. doi: 10.1016/s0896-6273(00)81150-2

Maccaferri, G., and Lacaille, J. C. (2003). Interneuron diversity series: hippocampal interneuron classifications-making things as simple as possible, not simpler. *Trends Neurosci.* 26, 564–571. doi: 10.1016/j.tins.2003.08.002

Manabe, T., and Nicoll, R. A. (1994). Long-term potentiation: evidence against an increase in transmitter release probability in the CA1 region of the hippocampus. *Science* 265, 1888–1892. doi: 10.1126/science.7916483

Manabe, T., Wyllie, D. J., Perkel, D. J., and Nicoll, R. A. (1993). Modulation of synaptic transmission and long-term potentiation: effects on paired pulse facilitation and EPSC variance in the CA1 region of the hippocampus. *J. Neurophysiol.* 70, 1451–1459.

Mann, E. O., and Paulsen, O. (2007). Role of GABAergic inhibition in hippocampal network oscillations. *Trends Neurosci.* 30, 343–349. doi: 10.1016/j.tins.2007.05.003

Marder, C. P., and Buonomano, D. V. (2003). Differential effects of short- and long-term potentiation on cell firing in the CA1 region of the hippocampus. *J. Neurosci.* 23, 112–121.

Markram, H., Lübke, J., Frotscher, M., Roth, A., and Sakmann, B. (1997). Physiology and anatomy of synaptic connections between thick tufted pyramidal neurones in the developing rat neocortex. *J. Physiol.* 500, 409–440. doi: 10.1113/jphysiol.1997.sp022031

McNaughton, B. L. (1980). Evidence for two physiologically distinct perforant pathways to the fascia dentata. *Brain Res.* 199, 1–19. doi: 10.1016/0006-8993(80)90226-7

McNaughton, B. L. (1982). Long-term synaptic enhancement and short-term potentiation in rat fascia dentata act through different mechanisms. *J. Physiol.* 324, 249–262. doi: 10.1113/jphysiol.1982.sp014110

Mehta, M. R., Lee, A. K., and Wilson, M. A. (2002). Role of experience and oscillations in transforming a rate code into a temporal code. *Nature* 417, 741–746. doi: 10.1038/nature00807

Nicoll, R. A., and Alger, B. E. (1979). Presynaptic inhibition: transmitter and ionic mechanisms. *Int. Rev. Neurobiol.* 21, 217–258. doi: 10.1016/s0074-7742(08)60639-x

Nishida, H., Takahashi, M., and Lauwereyns, J. (2014). Within-session dynamics of theta-gamma coupling and high-frequency oscillations during spatial alternation in rat hippocampal area CA1. *Cogn. Neurodyn.* 8, 363–372. doi: 10.1007/s11571-014-9289-x

O'Keefe, J., and Dostrovsky, J. (1971). The hippocampus as a spatial map. Preliminary evidence from unit activity in the freely-moving rat. *Brain Res.* 34, 171–175. doi: 10.1016/0006-8993(71)90358-1

O'Keefe, J., and Recce, M. L. (1993). Phase relationship between hippocampal place units and the EEG theta rhythm. *Hippocampus* 3, 317–330. doi: 10.1002/hipo.450030307

Paulsen, O., and Sejnowski, T. J. (2006). From invertebrate olfaction to human cognition: emerging computational functions of synchronized oscillatory activity. *J. Neurosci.* 26, 1661–1662. doi: 10.1523/jneurosci.3737-05a.2006

Pearce, R. A. (1993). Physiological evidence for two distinct GABA$_A$ responses in rat hippocampus. *Neuron* 10, 189–200. doi: 10.1016/0896-6273(93)90310-n

Pugliese, A. M., Ballerini, L., Passani, M. B., and Corradetti, R. (1994). EPSP-spike potentiation during primed burst-induced long-term potentiation in the CA1 region of rat hippocampal slices. *Neuroscience* 62, 1021–1032. doi: 10.1016/0306-4522(94)90340-9

Ranck, J. B. (1973). Studies on single neurons in dorsal hippocampal formation and septum in unrestrained rats. I. Behavioral correlates and firing repertoires. *Exp. Neurol.* 41, 461–531. doi: 10.1016/0014-4886(73)90290-2

Schulz, P. E., Cook, E. P., and Johnston, D. (1995). Using paired-pulse facilitation to probe the mechanisms for long-term potentiation (LTP). *J. Physiol. Paris* 89, 3–9. doi: 10.1016/0928-4257(96)80546-8

Sejnowski, T. J., and Paulsen, O. (2006). Network oscillations: emerging computational principles. *J. Neurosci.* 26, 1673–1676. doi: 10.1523/jneurosci.3737-05d.2006

Semyanov, A., Walker, M. C., Kullmann, D. M., and Silver, R. A. (2004). Tonically active GABA$_A$ receptors: modulating gain and maintaining the tone. *Trends Neurosci.* 27, 262–269. doi: 10.1016/j.tins.2004.03.005

Singer, W., and Gray, C. M. (1995). Visual feature integration and the temporal correlation hypothesis. *Annu. Rev. Neurosci.* 18, 555–586. doi: 10.1146/annurev.neuro.18.1.555

Smith, J., Lal, V., Bowser, D., Cappai, R., Masters, C., and Ciccotosto, G. (2009). Stimulus pattern dependence of the Alzheimer"s disease amyloid-beta 42 peptide's inhibition of long term potentiation in mouse hippocampal slices. *Brain Res.* 1269, 176–184. doi: 10.1016/j.brainres.2009.03.007

Song, S., Miller, K. D., and Abbott, L. F. (2000). Competitive Hebbian learning through spike-timing-dependent synaptic plasticity. *Nat. Neurosci.* 3, 919–926. doi: 10.1038/78829

Staff, N. P., and Spruston, N. (2003). Intracellular correlate of EPSP-spike potentiation in CA1 pyramidal neurons is controlled by GABAergic modulation. *Hippocampus* 13, 801–805. doi: 10.1002/hipo.10129

Stent, G. S. (1973). A physiological mechanism for Hebb's postulate of learning. *Proc. Natl. Acad. Sci. U S A* 70, 997–1001. doi: 10.1073/pnas.70.4.997

Suh, J., Rivest, A. J., Nakashiba, T., Tominaga, T., and Tonegawa, S. (2011). Entorhinal cortex layer III input to the hippocampus is crucial for temporal association memory. *Science* 334, 1415–1420. doi: 10.1126/science.1210125

Thompson, L. T., and Best, P. J. (1989). Place cells and silent cells in the hippocampus of freely-behaving rats. *J. Neurosci.* 9, 2382–2390.

Tiesinga, P., Fellous, J. M., and Sejnowski, T. J. (2008). Regulation of spike timing in visual cortical circuits. *Nat. Rev. Neurosci.* 9, 97–107. doi: 10.1038/nrn2315

Tominaga, Y., Ichikawa, M., and Tominaga, T. (2009). Membrane potential response profiles of CA1 pyramidal cells probed with voltage-sensitive dye optical imaging in rat hippocampal slices reveal the impact of GABA(A)-mediated feed-forward inhibition in signal propagation. *Neurosci. Res.* 64, 152–161. doi: 10.1016/j.neures.2009.02.007

Tominaga, T., and Tominaga, Y. (2010). GABA$_A$ receptor-mediated modulation of neuronal activity propagation upon tetanic stimulation in rat hippocampal slices. *Pflugers Arch.* 460, 875–889. doi: 10.1007/s00424-010-0870-9

Tominaga, T., Tominaga, Y., and Ichikawa, M. (2002). Optical imaging of long-lasting depolarization on burst stimulation in area CA1 of rat hippocampal slices. *J. Neurophysiol.* 88, 1523–1532. doi: 10.1152/jn.00554.2001

Tominaga, T., Tominaga, Y., and Yamada, H. (2000). Quantification of optical signals with electrophysiological signals in neural activities of Di-4-ANEPPS stained rat hippocampal slices. *J. Neurosci. Methods* 102, 11–23. doi: 10.1016/s0165-0270(00)00270-3

Wakita, M., Kotani, N., Kogure, K., and Akaike, N. (2014). Inhibition of excitatory synaptic transmission in hippocampal neurons by levetiracetam involves Zn^{2+}-dependent GABA type A receptor-mediated presynaptic modulation. *J. Pharmacol. Exp. Ther.* 348, 246–259. doi: 10.1124/jpet.113.208751

Watanabe, S., Hoffman, D. A., Migliore, M., and Johnston, D. (2002). Dendritic K^+ channels contribute to spike-timing dependent long-term potentiation in hippocampal pyramidal neurons. *Proc. Natl. Acad. Sci. U S A* 99, 8366–8371. doi: 10.1073/pnas.122210599

White, J. A., Banks, M. I., Pearce, R. A., and Kopell, N. J. (2000). Networks of interneurons with fast and slow gamma-aminobutyric acid type A (GABA$_A$) kinetics provide substrate for mixed gamma-theta rhythm. *Proc. Natl. Acad. Sci. U S A* 97, 8128–8133. doi: 10.1073/pnas.100124097

Yamamoto, J., Suh, J., Takeuchi, D., and Tonegawa, S. (2014). Successful execution of working memory linked to synchronized high-frequency gamma oscillations. *Cell* 157, 845–857. doi: 10.1016/j.cell.2014.04.009

Zhu, G., Liu, Y., Wang, Y., Bi, X., and Baudry, M. (2015). Different patterns of electrical activity lead to long-term potentiation by activating different intracellular pathways. *J. Neurosci.* 35, 621–633. doi: 10.1523/JNEUROSCI.2193-14.2015

Conflict of Interest Statement: The authors declare that the research was conducted in the absence of any commercial or financial relationships that could be construed as a potential conflict of interest.

SCIENTIFIC REPORTS

OPEN

Received: 05 December 2014
Accepted: 24 June 2015
Published: 28 July 2015

Double strand break repair by capture of retrotransposon sequences and reverse-transcribed spliced mRNA sequences in mouse zygotes

Ryuichi Ono[1,2,*], Masayuki Ishii[2,*], Yoshitaka Fujihara[3], Moe Kitazawa[2], Takako Usami[4], Tomoko Kaneko-Ishino[5], Jun Kanno[1], Masahito Ikawa[3] & Fumitoshi Ishino[2,6]

The CRISPR/Cas system efficiently introduces double strand breaks (DSBs) at a genomic locus specified by a single guide RNA (sgRNA). The DSBs are subsequently repaired through non-homologous end joining (NHEJ) or homologous recombination (HR). Here, we demonstrate that DSBs introduced into mouse zygotes by the CRISPR/Cas system are repaired by the capture of DNA sequences deriving from retrotransposons, genomic DNA, mRNA and sgRNA. Among 93 mice analysed, 57 carried mutant alleles and 22 of them had long *de novo* insertion(s) at DSB-introduced sites; two were spliced mRNAs of *Pcnt* and *Inadl* without introns, indicating the involvement of reverse transcription (RT). Fifteen alleles included retrotransposons, mRNAs, and other sequences without evidence of RT. Two others were sgRNAs with one containing T7 promoter-derived sequence suggestive of a PCR product as its origin. In conclusion, RT-product-mediated DSB repair (RMDR) and non-RMDR repair were identified in the mouse zygote. We also confirmed that both RMDR and non-RMDR take place in CRISPR/Cas transfected NIH-3T3 cells. Finally, as two *de novo* MuERV-L insertions in C57BL/6 mice were shown to have characteristic features of RMDR in natural conditions, we hypothesize that RMDR contributes to the emergence of novel DNA sequences in the course of evolution.

Whole genome sequencing of a number of different mammalian species has established that approximately 50% of the mammalian genome is derived from transposable elements[1–3]. Retrotransposons, which mobilize via an RNA intermediate by a copy-and-paste mechanism, comprise the majority of mammalian transposable elements, whereas DNA transposons, which move via a cut-and-paste mechanism, comprise a relatively small fraction, having accumulated mutations that render them immobile[4].

[1]Division of Cellular and Molecular Toxicology, Biological Safety Research Centre, National Institute of Health Sciences (NIHS), 1-18-1 Kamiyoga, Setagaya-ku, Tokyo, 158-8501, Japan. [2]Department of Epigenetics, Medical Research Institute, Tokyo Medical and Dental University, 1-5-45 Yushima, Bunkyo-ku, Tokyo 113-8510, Japan. [3]Research Institute for Microbial Diseases, Osaka University, Suita, Osaka 565-0871, Japan. [4]Facility for Recombinant Mice, Medical Research Institute, Tokyo Medical and Dental University, 2-3-10 Kandasurugadai, Chiyoda-ku, Tokyo 101-0062, Japan. [5]School of Health Sciences, Tokai University, 143 Shimokasuya, Isehara, Kanagawa 259-1193, Japan. [6]Global Centre of Excellence Programme for International Research Centre for Molecular Science in Tooth and Bone Diseases, Tokyo Medical and Dental University, 1-5-45 Yushima, Bunkyo-ku, Tokyo 113-8510, Japan. *These authors contributed equally to this work. Correspondence and requests for materials should be addressed to R.O. (email: onoryu@nihs.go.jp) or (email: ono-ryuichi@umin.ac.jp)

Retrotransposons can be subdivided into two classes, long terminal repeat (LTR) retrotransposons and non-LTR retrotransposons[4,5]. LTR retrotransposons contain two LTRs, they encode the proteins Gag and Pol with activities similar to those of simple retroviruses such as protease, reverse transcriptase and integrase activities, but they lack an envelope (*Env*) gene. The LTRs are direct sequence repeats that contain a promoter recognized by the host RNA polymerase II to produce the retrotransposon mRNA. The Gags are structural proteins that form the virus-like particle, inside of which RT takes place. The reverse transcriptase copies its mRNA into a cDNA, and the integrase inserts the cDNA into a new target site. The cleavages of the two strands at the target site are staggered, resulting in target-site duplications (TSDs)[4,5]. Long interspersed elements (LINEs), a type of non-LTR retrotransposon, lack LTRs and encode two open reading frames (ORFs). These elements mobilize by target-site-primed reverse transcription (TPRT). TPRT is a mechanism by which an element-encoded endonuclease generates a single-strand nick in the genomic DNA, liberating a 3′OH that is used to prime reverse transcription of the RNA. The integration site formed by TPRT is usually flanked by TSDs[4,5]. The endonuclease and reverse transcriptase activities of non-LTR retrotransposons also have the ability to mobilize other non-autonomous short interspersed elements (SINEs)[6–8], and certain classes of non-coding RNAs[9–12] and mRNAs[13,14], which can result in the formation of processed pseudogenes.

Retrotransposons continue to sculpt mammalian genomes and behave as insertional mutagens, either by disrupting exons or by insertion into introns, leading to mis-splicing[5,15,16]. Hence, retrotransposons occasionally have deleterious effects on host genes and thus organisms. However, a growing body of evidence suggests that retrotransposons and retrotransposon-derived genes have also acquired functions essential for host survival during mammalian evolution including placental formation, neurogenesis and gene regulation[17–25].

Recent studies have shown that a large number of different retrotransposon families are highly transcribed in the mouse zygote, and in fact, they produce cDNAs by reverse transcription (RT)[26–29]. In *Saccharomyces cerevisiae,* the capture of Ty1 retrotransposon cDNA at the site of DSBs has been observed when homologous recombination is blocked[30,31]. It was thus reasoned that RT-product-mediated DSB repair (RMDR) is functional in the mouse zygote because of its high RT activity.

DSBs result from both exogenous insults (e.g., reactive oxygen species, irradiation, chemical agents and ultraviolet light) and endogenous cellular events (e.g., transposition, meiotic double strand break formation)[5,32,33]. The clustered regularly interspaced short palindromic repeat (CRISPR)/Cas system has made it possible to induce double strand breaks (DSBs) at specific loci in the mammalian genome[34–39]. In this report, DSBs were introduced into 8 genomic loci of the mouse zygote, the *Peg10-ORF1* and *Peg10-ORF2* regions and the *Cxx1a*, *Cxx1b*, *Rgag1*, *Rsph6a*, *Spaca5* and *Ddx3y* genes. We analysed the sequences of the DSB-induced sites to determine whether RMDR was at work. We also introduced DSBs into NIH-3T3 cells to assess the universality of the phenomenon, doing so with or without an RT-inhibitor to determine whether RMDR could be inhibited.

Results

DSBs were introduced by CRISPR/Cas into mouse zygotes. Single guide RNAs (sgRNAs) were designed for each of the eight target genomic loci, and the DSB induction efficiency was validated with an EGxxFP system[40] (Fig. 1a). We confirmed that all the sgRNAs were able to induce fluorescent cells at more than 30% efficiency (Fig. 1b, Supplementary Fig. 1). It was previously reported that more than 30% efficiency obtained with an EGxxFP system allows for the stable generation of mutant mice by injecting the sgRNA sequence for each gene along with the hCas9 gene as an RNA or a plasmid (with oligo DNAs for the knock-in mice) into fertilized eggs[40]. Mutant and knock-in mice were obtained by CRISPR/Cas injection under various conditions (Supplementary Table 1,2). The pups and embryos that developed from these embryos were subjected to PCR and subsequent sequence analysis (Fig. 1c, Supplementary Table 1,2). CRISPR/Cas-mediated mutant mice (including mosaicism mutations) were obtained with high efficiency (23.1% to 100%) from all the different sgRNAs used (Fig. 1b, Supplementary Fig. 1). In total, 61% (57 out of 93) of the embryos or pups carried a CRISPR/Cas-mediated mutant allele, suggesting that the DSB induction activity is adequate in these mouse zygotes and validating the EGxxFP system (Supplementary Table 1,2, Fig. 1b, Supplementary Fig. 1). However, we found that 22 pups and embryos had extra unknown PCR products larger than the expected length (Fig. 1c, Supplementary Table 1,2). We isolated these extra PCR products after electrophoresis, and 20 out of 22 PCR products had their sequences successfully determined (Supplementary Table 1,2). These PCR products were found to have *de novo* insertions of retrotransposons, genomic DNA, mRNA and sgRNA sequence at the DSB-induced loci. These data demonstrate that, at least in the case of two insertions of mRNA sequences, i.e., *Pcnt* and *Inadl*, which are missing introns, RMDR is functional in mouse zygotes.

DSBs were repaired by the capture of retrotransposon sequences. Detailed characterization of the *de novo* insertions at the target DSB sites in the *Peg10*-ORF2 coding region revealed that two of the animals (*Peg10*-ORF2-#8 and *Peg10*-ORF2-#18) had 327-bp and 357-bp insertions of the murine endogenous retrovirus-L (MuERV-L, also known as the MERVL or Erv4) Pol protein coding region[26] (Fig. 2a,c). MuERV-L is an endogenous retrovirus that is one of the most abundant transcripts in the 2-cell stage embryo[26–29]. In each case, there were small overlapping nucleotides called "microhomologies" between the inserted retrotransposon and the DSB-induced target site, and truncations of both the

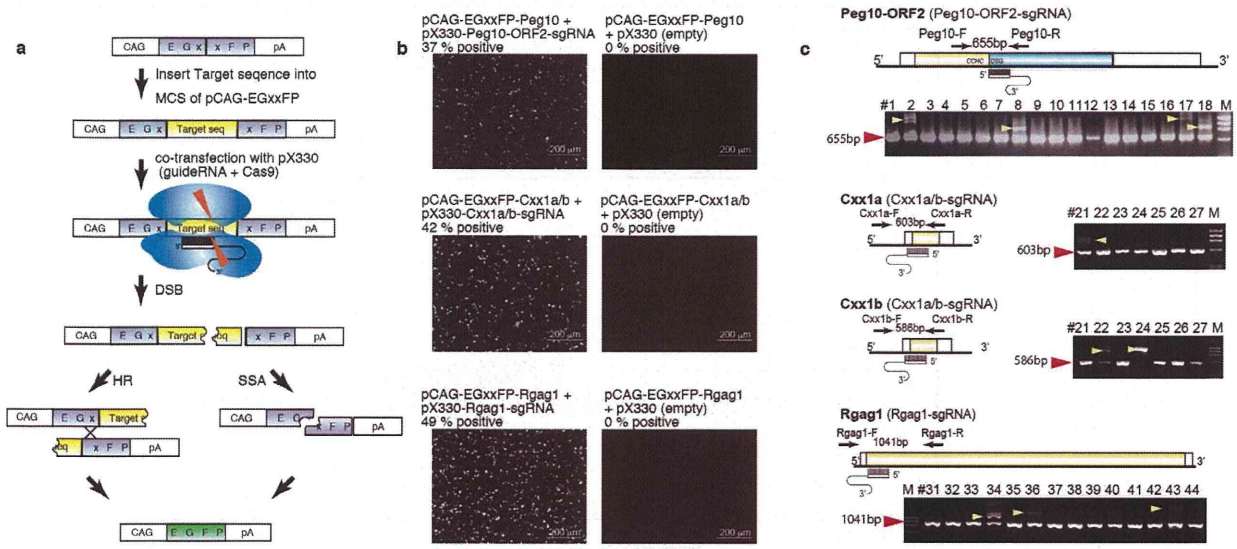

Figure 1. CRISPR/Cas mediated gene manipulation. (**a**) The pCAG-EGxxFP plasmid contains 5′ and 3′ EGFP fragments that share 482 bp under a ubiquitous CAG promoter. A 500-bp genomic fragment containing the sgRNA target sequence was placed between the EGFP fragments of the pCAG-EGxxFP plasmid. The resulting target plasmid was co-transfected with pX330 plasmids expressing the sgRNA and hCas9 into HEK293T cells. Once the target sequence was digested by sgRNA guided CAS9 endonuclease, homology dependent repair (HR: homologous recombination, or SSA: single-strand annealing) took place and reconstituted the EGFP expression cassette. MCS; multi cloning site. (**b**) The DSB efficiency was validated with the pCAG-EGxxFP system by observing EGFP fluorescence 48 hrs after the transfection (scale bar: 200 μm). The percentages of EGFP-positive cells are indicated. (**c**) Schematic representation of the positions of each sgRNA and primer to check the CRISPR/Cas mediated mutations (left side of (**c**)). Electrophoresis of the PCR products from each of the pX330 plasmid-injected mice (the right side of (**c**)). At least four PCR products (yellow arrowheads) were larger than expected (WT: red arrowheads) in the *Peg10*-ORF2-sgRNA-injected mice. One and two PCR products (yellow arrowheads) were larger than *Cxx1a* WT and *Cxx1b* WT, respectively, in the *Cxx1a/b*-sgRNA-injected pups. Three PCR products (yellow arrowheads) were larger than 1041 bp (*Rgag1* WT) in the *Rgag1*-sgRNA-injected pups.

5′ and 3′ regions of the inserted retrotransposon including the LTRs were present, suggest that these LTR retrotransposons had not been integrated by typical replicative retrotransposition[41–46]. Furthermore, the *Peg10*-ORF2-#17 animal was found to have a 950-bp insertion of a partial internal region and a truncated LTR of the retrovirus-like element MaLR, which is the second most abundant retrotransposon transcript in the 2-cell stage mouse embryo[29] (Fig. 2b).

To the best of our knowledge, this is the first direct evidence of the introduction of MuERV-L and MaLR retrotransposons at a specifically desired genomic locus in mouse zygotes. Because MaLR does not encode any known protein and its means of propagation in the genome is unknown, it has been suggested that the RT activity of MuERV-L might be the means of its propagation[27,28]. Insertions of partial retrotransposon sequences with microhomologies were also observed at all of the target DSB sites introduced (Fig. 2d–f, Supplementary Fig. 2a–c,e,g–j). Although the DSB-induced loci were different, the same types of endogenous retroviruses were inserted at each locus, indicating that the capture of retrotransposon sequences may occur at any DSB site in the mouse zygote. Furthermore, there was a case in which an allele had multiple retrotransposon insertions at the same DSB site (Fig. 2e). Each of the junction sequences between the retrotransposons has 1–5 bp of complete overlapping microhomology.

DSBs were repaired by the capture of RT-mediated cDNA. In addition to retrotransposon sequences there were also mRNA sequence insertions at the DSB-induced loci. *De novo* insertions at *Peg10* ORF2, *Peg10* ORF1 and *Spaca5* included mRNA sequence-derived partial sequences of the *Pcnt* (*Pericentrin*) gene (Fig. 3a), *Inadl* (*InaD-like*) gene (Fig. 3b), *Cpd* (*carboxypeptidase D*) gene (Supplementary Fig. 2b), *Tpm3* (*tropomyosin 3, gamma*) gene (Supplementary Fig. 2c), *Zfp609* (*zinc finger protein 609*) gene (Supplementary Fig. 2d), *Actr2* (*ARP2 actin-related protein 2*) gene (Supplementary Fig. 2j) and *Peg10* gene (Fig. 2a, Supplementary Fig. 2a). Expression of the *Pcnt, Inadl, Cpd, Tpm3, Zfp609, Actr2* and *Peg10* genes was confirmed at the 2- to 16-cell embryonic stages[29,47,48], and the inserted partial *Pcnt* and *Inadl* sequences correspond to the 6803–7599 bp and 1527–1836 bp regions of the full length *Pcnt* and *Inadl* mRNAs, respectively, skipping *Pcnt* intron 30–32 and *Inadl* intron 11–14, demonstrating that

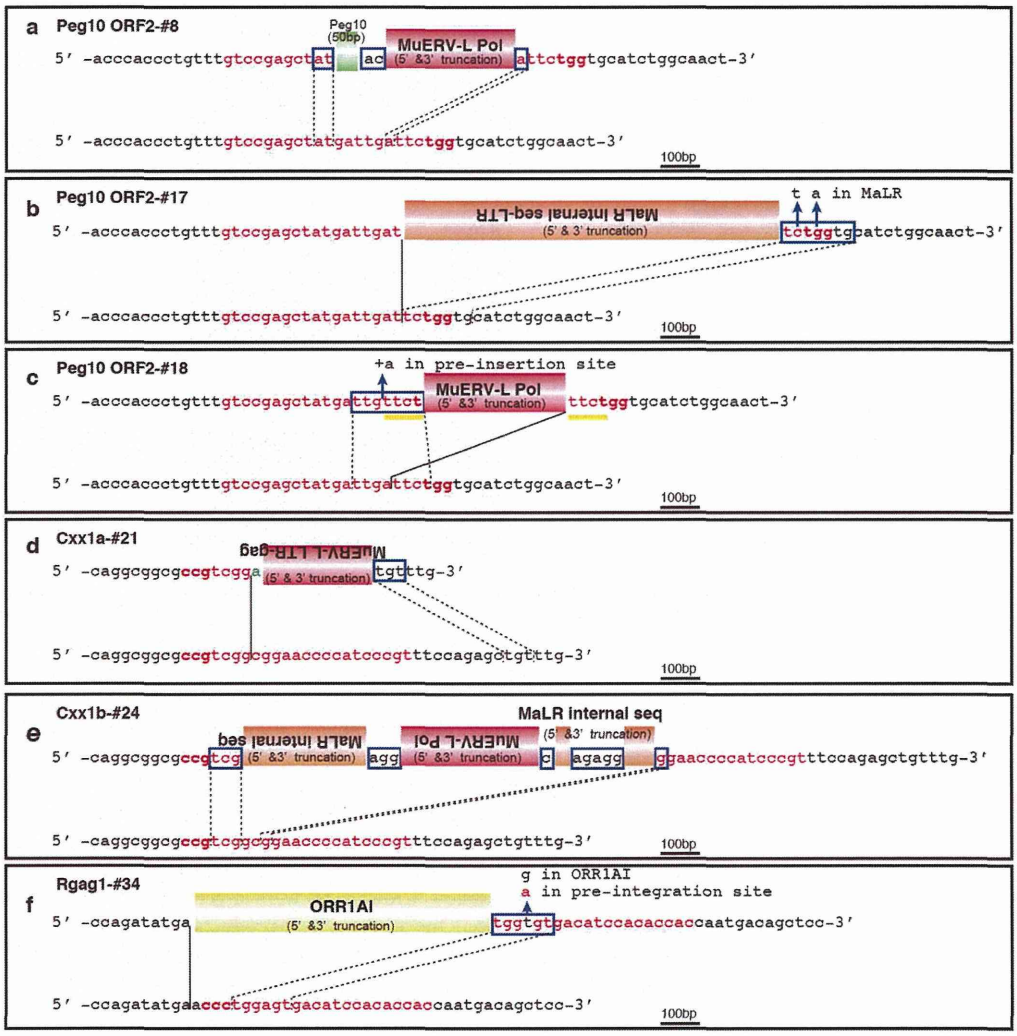

Figure 2. Structure of the captured retrotransposons associated with DSB repair. *De novo* inserted retrotransposons at the *Peg10*-ORF2 (**a–c**), *Cxx1a/b* (**d**,**e**), and *Rgag1* (**f**) loci were induced by pX330 injection into mouse zygotes. Both the post-integration site and pre-integration sequences (bottom of the panel) are shown. The nucleotide sequences that correspond to the single guide RNA sequence and the PAM sequences are shown in red and bold red characters, respectively. The black lines indicate the junction sites between pre- and post-integration sequences. The sequences in the blue boxes are overlapping microhomologies and are marked with black dotted lines. Short sequences of unknown origin are shown in green. Each insertion was truncated at both the 5′ and 3′ ends, but they demonstrated distinct features. These included the absence of LTRs and TSDs. (**a**) Together with MuERV-L, 50 bp of *Peg10* cDNA sequence was inserted with 1-bp microhomology. (**b**) A truncated MaLR internal sequence was inserted with a 7-bp overlapping microhomology (a 2-bp mismatch). (**c**) A truncated MuERV-L Pol region was inserted with a 7-bp microhomology (1-bp mismatch) and 4-bp TSDs (yellow bars) 'ttct'. (**d**) A truncated MuERV-L was inserted with 3-bp overlapping microhomology. (**e**) Multiple truncated retrotransposons were inserted with 1-5-bp microhomologies. (**f**) A truncated ORR1AI retrotransposon was inserted with a 6-bp microhomology (1-bp mismatch).

these partial *Pcnt* and *Inadl* insertions are mediated by RMDR. The sequences flanking the insertions have no polyA tails for any of the captured genes, but short microhomology is present for *Pcnt, Cpd, Tpm3, Zfp609, Actr2* and *Peg10*, supporting the notion that the cDNA gene formation is not mediated by conventional TPRT pathways[14,49–52] but rather by RMDR (Fig. 4c,d).

The mouse with the *Inadl* insertion was produced in the process of obtaining knock-in (KI) mice with a point mutation in the CCHC zinc finger domain of Peg10 ORF1 by CRISPR/Cas co-injection with DNA oligos. The DNA oligos have 53 bp and 80 bp homologous regions and a T to G point mutation near the DSB site. As a result, 5 pups (#53, #54, #55, #61 and #62 in Table S1) were born with the KI